PERGAMON

International Journal of Heat and Mass Transfer 41 (1998) 3109–3120

International Journal of HEAT and MASS TRANSFER

Heat and mass transfer for plate fin-and-tube heat exchangers, with and without hydrophilic coating

Chi-Chuan Wang[a,*], Chang-Tsair Chang[b]

[a] *Energy & Resources Laboratories, Industrial Technology Research Institute, Hsinchu, Taiwan*
[b] *Yuan-Ze University, Chungli, Taiwan*

Received 24 December 1997

Abstract

Heat and mass transfer characteristics of fin-and-tube heat exchangers with and without hydrophilic coating were reported in this study. The test exchangers consisted of three different louvre fin patterns and their corresponding plain fin counterpart. For completely dry test conditions, the enhancement level for the enhanced fin pattern decreases with increase of fin pitch. The Gray and Webb correlation considerably under-predicts the present 7.0 and 9.5 mm tube diameter plain fin samples. For dehumidifying test conditions, the effect of hydrophilic coating on the sensible heat transfer coefficients is negligible, and there are no detectable changes of the sensible heat transfer coefficients with change of inlet relative humidity. However, the pressure drops for the hydrophilic coated surfaces are sensitive to the inlet relative humidity.

Key words: Augmentation; Heat exchangers; Finned surfaces.

Nomenclature

A_c minimum free flow area [m^2]
A_o total surface area [m^2]
D_c tube outside diameter, include collar thickness [m]
D_h hydraulic diameter, 4 $A_c L/A_o$ [m]
f friction factor, dimensionless
F_p fin pitch [mm]
$h_{c,o}$ sensible heat transfer coefficient for wet coils [W m^{-2} K^{-1}]
h_d mass transfer coefficient [kg m^{-2} s^{-1}]
h_{louver} sensible heat transfer coefficient for louver fin pattern [W m^{-2} K^{-1}]
h_{plain} sensible heat transfer coefficient for plain fin pattern [W m^{-2} K^{-1}]
$i_{air,in}$ air enthalpy evaluated at heat exchanger inlet [kJ kg^{-1}]
$i_{air,out}$ air enthalpy evaluated at heat exchanger outlet [kJ kg^{-1}]
$i_{g,t}$ enthalpy of saturated water vapor evaluated at mean air temperature [kJ kg^{-1}]
j the Colburn factor, dimensionless
j_4 the Colburn factor for 4-row coil, dimensionless
j_N the Colburn factor for N-row coil, dimensionless
L heat exchanger depth [m]
L_p Louver pitch [mm]
$\dot{m}_a$ air mass flow rate [kg s^{-1}]
$\dot{m}_w$ water mass flow rate [kg s^{-1}]
N the number of tube row
ΔP pressure drop [Pa]
P_l longitudinal tube pitch [mm]
Pr Prandtl number, dimensionless
P_t transverse tube pitch [mm]
$\dot{Q}_{avg}$ mathematical average heat transfer rate for $\dot{Q}_w$ and $\dot{Q}_a$ [kW]
$\dot{Q}_a$ air side heat transfer rate [kW]
$\dot{Q}_w$ water side heat transfer rate [kW]
p system pressure [Pa]
p_{AI} partial air pressure evaluated at the condensate interface [Pa]
Re_{D_h} Reynolds number based in hydraulic diameter, D_h
Re_{D_c} Reynolds number based on D_c
RH relative humidity, dimensionless
s fin spacing, [mm]
Sc Schmidt number, dimensionless
T temperature [°C]

* Corresponding author. Tel.: 00-886-35-916294; fax: 00-886-35-820250; e-mail: f781058@erlb.erl.itri.org.tw.

0017-9310/98 $19.00
PII: S0017-9310(98)00060-X

$U_{o,w}$ overall heat transfer coefficient with wet condition
V_{fr} frontal velocity [m s^{-1}]
W humidity ratio [kg kg^{-1} dry air]
$W_{air,in}$ humidity ratio evaluated at heat exchanger inlet [kg kg^{-1} dry air]
$W_{air,in}$ humidity ratio evaluated at heat exchanger outlet [kg kg^{-1} dry air]
$W_{s,w}$ humidity ratio of saturated moist air evaluated at condensate temperature [kg kg^{-1} dry air].

Greek symbols
δ fin thickness [m]
ρ_{AI} saturated air density evaluate at the condensate interface [kg m^{-3}]
ρ_{AO} mean air density evaluate at the bulk temperature [kg m^{-3}].

1. Introduction

Fin-and-tube heat exchangers are widely used in air-conditioners operating as evaporators and condensers. These heat exchangers consist of mechanically or hydraulically expanded round tubes in a block of parallel continuous fins. For commerical application, the tubes used in the fin-and-tube heat exchangers are generally 12.7 or 15.88 mm. For household applications, the tube size could be less than 10 mm, usually 9.52 mm, and recently, even 7.0 mm in residential application. This is because higher heat transfer coefficients and lower pressure drops can be achieved by using smaller tubes, and eventually led to much more compact fin-and-tube heat exchangers design. This is especially helpful in space-limited areas. Thus the use of 7.0 mm tube along with small longitudinal and transverse pitch (12.7 and 21 mm) fin-and-tube heat exchangers has become popular.

There are many variants of the fin pattern for fin-and-tube heat exchangers, and louver fin and plain fin are among the most popular used in residential air-conditioners. Extensive data for several louver fin geometries having 9.52 and 7.94 mm tubes (P_t = 25.4 mm, P_l = 19.05 mm) were recently reported by Chang et al. [1], and Wang et al. [2, 3]. Experimental data for smaller longitudinal and transverse tube pitch that use 7 mm tube; however, is very rare for both louver and plain fin.

The present study involves tests for both dry and wet operation conditions. For wet operating conditions, the surface temperatures of the fins are always below the dew point temperature. Consequently, moisture is condensed on the fins. Since water condensate typically has a high contact angle on the aluminium fins, the water may adhere as droplets, causing bridging between the fins, and increase air pressure drop. Furthermore, the agglomerated water condensate may corrode aluminium fins, and produces corrosion problems. Therefore if the water contact angle can be further reduced, condensate drainage will be improved. This will allow the use of smaller fin pitch, and possibly higher air velocities to achieve higher heat transfer performance. A solution to this problem is to use hydrophilic coating on the aluminium fins. The hydrophilic coating can effectively reduce the contact angle of water condensate and improve the condensate drainage. Information on the hydrophilic coating on the thermal/hydraulic performances of the fin-and-tube heat exchangers is very rare in the open literature. Only two researches relating to the hydrophilic coating are available at present.

Mimaki [4] showed that the air-side heat transfer coefficient of the coated surfaces is approximately the same with those of uncoated cores, and a 20–50% lower pressure drop for the hydrophilic coating cores under fully wet conditions were reported. Hong [5] presented a fundamental aspect to the hydrophilic coating surfaces. As shown, heat/mass transfer characteristics for hydrophilic coating is rare, the available literature on the dehumidifying heat exchangers still offers limited information to assist the designer in designing the heat exchangers. Therefore, the objective of the present study is to provide systematic experimental information on the air-side performance of fin-and-tube heat exchangers having smaller tube size, longitudinal, transverse tube pitch under dry and wet conditions.

2. Experimental apparatus and data reductions

A total of eleven fin-and-tube heat exchangers were tested in this study, and their detailed geometrical parameters are tabulated in Table 1. The test samples include three kinds of enhanced fin patterns and a plain fin pattern. Detailed drawings of the present enhanced fin patterns are given in Fig. 1a (parallel louver), Fig. 1b (louver), and Fig. 1c (louver). The test fin-and-tube heat exchangers are tension wrapped having a 'L' type fin collar. Thermal contact resistance provided by the manufacturers to the total resistance to the test coils are estimated to be less than 3% throughout the test. The test conditions are as follows:

Dry-bulb temperatures of the air:	27 ± 0.5°C
Inlet relative humidity for the incoming air:	50% and 85%
Inlet air velocity:	0.3–8 m s^{-1} (for dry operation) 0.3–4.0 m s^{-1} (for wet operation)
Inlet water temperature	60 ± 1.0°C (for dry operation) 7 ± 0.5°C (for wet operation)
Water velocity inside the tube	2.5–3.0 m s^{-1}

Two kinds of hydrophilic coating were tested and com-

Table 1
Geometric dimensions of the sample plate fin-and-tube heat exchangers

No	Fin pattern	Fin pitch, F_p (mm)	Nominal tube O.D. (mm)	D_c (mm)	P_t (mm)	P_l (mm)	Surface treatment	Row number
1	Plain	1.4	7	7.52	20.4	12.7	Nil	2
2	Parallel Louver (Fig. 1a)	1.4	7	7.52	20.4	12.7	Nil	2
3	Parallel Louver (Fig. 1a)	1.4	7	7.52	20.4	12.7	Hydrophilic coating (pre-coated)	2
4	Parallel Louver (Fig. 1a)	1.4	7	7.52	20.4	12.7	Hydrophilic coating (Cosmer)	2
5	Plain	1.4	9.52	10.23	20.4	16.7	Nil	2
6	Plain	1.4	9.52	10.23	20.4	16.7	Hydrophilic coating (Cosmer)	2
7	Louver (Fig. 1b)	1.4	9.52	10.23	20.4	16.7	Nil	2
8	Plain	1.71	7	7.52	21.0	12.7	Nil	2
9	Louver (Fig. 1c)	1.71	7	7.52	21.0	12.7	Hydrophilic coating (pre-coated)	2
10	Plain	1.22	7	7.52	21.0	12.7	Nil	2
11	Louver (Fig. 1c)	1.22	7	7.52	21.0	12.7	Hydrophilic coating (pre-coated)	2

Note: D_c is the tube outside diameter (including collar thickness) after expansion ($D_c = D_o + 2\delta_f$)

pared, namely, the pre-coated and Cosmer coating. The Cosmer coating is a dipping process which involved typical process treatments of the assembled heat exchangers by successively immersing the heat exchangers into a series of chemical solution, consisting 23% ethylene glycol monobutyl ether, 9% acrylic resin, 0.7% of NH_3, and 67.3% of water. The other hydrophilic coating heat exchanger has a pre-coated surface which is a two-layer surface coating as shown in Fig. 2. The base surface is aluminium, and the first layer involves anti-corrosion treatment, and the hydrophilic coating for the second layer. Schematic diagram of the experimental facility is shown in Fig. 3. The test facility is constructed based on several standards including ASHRAE standard 41.1, 41.2, and 38 [6, 7, 8]. In the experiments, only those data that satisfy the ASHRAE 33–78 requirements, (namely the energy balance conditions, $|\dot{Q}_w - \dot{Q}_a|/\dot{Q}_{avg}$ is less than 0.05), are used in the final analysis. The $\dot{Q}_w$ and $\dot{Q}_a$ is the water- and air-side heat transfer rate, respectively. The $\dot{Q}_{avg}$ is the mathematical average heat transfer rate for $\dot{Q}_w$ and $\dot{Q}_a$. Uncertainties reported in the present investigation, following the single-sample analysis proposed by Moffat [9], are tabulated in Table 2. The corresponding reduction method under completely dry conditions can be found from several previous studies (Wang et al. [10, 11]).

For wet coils, the overall heat transfer coefficient, $U_{o,w}$, in the present study is based on the enthalpy potential (Threlkeld [12]); detailed reduction of the sensible heat transfer coefficients is given by Wang et al. [11].

The determination of the mass transfer coefficient can be obtained from the process line (Threlkeld [12]), namely,

$$\frac{di}{dW} = Le\,\frac{i - i_W}{W - W_{S,W}} + (i_{g,t} - 2500.9 \times Le) \tag{1}$$

where the parameter, Le, is given as

$$Le = \frac{h_{c,o}}{h_d C_{p,a}}. \tag{2}$$

Detailed evaluation procedure of the mass transfer coefficients is as follows (Myers [13]):

(1) Obtaining the sensible heat transfer coefficient from the test data using the reduction methods described by Wang et al. [11].
(2) Assume a value of Le for a prescribed inlet condition.
(3) For a prescribed inlet condition ($i_{air,in}$, $W_{air,in}$), integrate equation (1) from inlet to outlet to achieve the outlet enthalpy, $i_{air,out}$.
(4) Check the value of $W_{air,out}$ and the experimental data. If the value is not equal to the experimental data, repeat step (2).
(5) Obtain mass transfer coefficient, h_d, from equation (2).

3. Results and discussion

The experimentally determined values of the Colburn j factor and friction factor f for the plate fin-and-tube

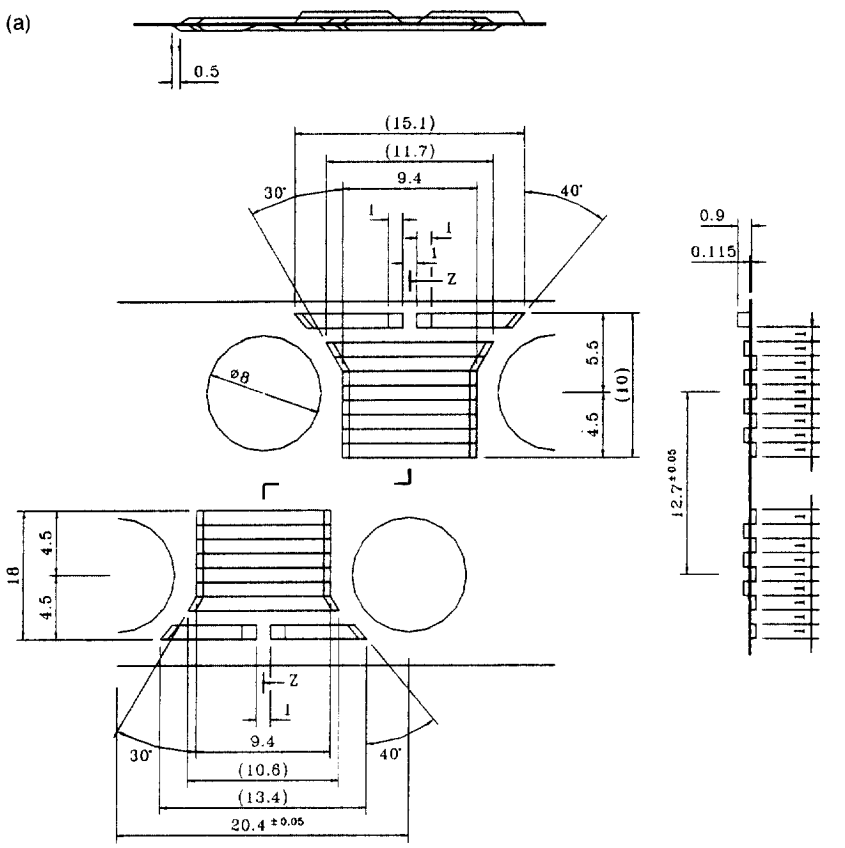

Fig. 1a. Detailed configuration of lanced fin pattern (samples #2, #3, and #4).

heat exchangers having plain fin geometry (sample #1, #5, #6, and #8, #10) plotted against Reynolds number (Re_{D_c}) are displayed in Fig. 4. The characteristics dimension for the Reynolds number, Re_{D_c}, is the tube outside diameter including collar thickness ($D_c = D_o + 2\delta_f$). Also shown in Fig. 4 are the calculated results for samples #1, #5, and #10, based on the Gray and Webb correlation [14]. As seen, for $Re_{D_c} = 2000$, the Gray and Webb correlation gives fairly good predictions of the friction factors (especially for 7 mm tube). However, considerable under-predictions of the heat transfer performance are seen compared to the present test data. For $Re_{D_c} < 1000$ (corresponds to air velocity V_{fr} of 1 m s^{-1}), the under-predictions may be more than 100%, and a 40% under-prediction is seen for $Re_{D_c} > 5000$ ($V_{fr} > 4.5$ m s^{-1}). Examination of the data bank of Gray and Webb and the present test data indicates the Gray and Webb [14] correlation may be more appropriate for larger tube diameter and larger longitudinal pitch. This is because the Gray and Webb correlation was developed from a database of tube diameters larger than the present work. The original Gray and Webb correlation [14] for heat transfer is quoted here as:

$$j_4 = 0.14 Re_{D_c}^{-0.328} \left(\frac{P_t}{P_l}\right)^{-0.502} \left(\frac{s}{D_c}\right)^{0.0312} \tag{3}$$

and

$$\frac{j_N}{j_4} = 0.991 \left[2.24 Re_{D_c}^{-0.092} \left(\frac{N}{4}\right)^{-0.031}\right]^{0.607(4-N)} \tag{4}$$

For most of the samples used by Gray and Webb the parameters, P_l/D, are within 2.1–2.6 compared to 1.54–1.63 for the present geometry. It seems that P_l/D may play an important role in correlating the data. To extend the applicability of the Gray and Webb correlation [14], and without the loss of generality, equation (3) is modified by multiplying a parameter of $2.55(P_l/D_c)^{-1.28}$ to become

$$j_4 = 0.357 Re_{D_c}^{-0.328} \left(\frac{P_t}{P_l}\right)^{-0.502} \left(\frac{s}{D_c}\right)^{0.0312} \left(\frac{P_t}{D_c}\right)^{-1.28} \tag{5}$$

This modified j_4 was calculated to compare Rich's test data [15, 16] and the present test data. Tables 3 and 4 show a comparison between the Gray and Webb correlation and the present modified correlation. As seen,

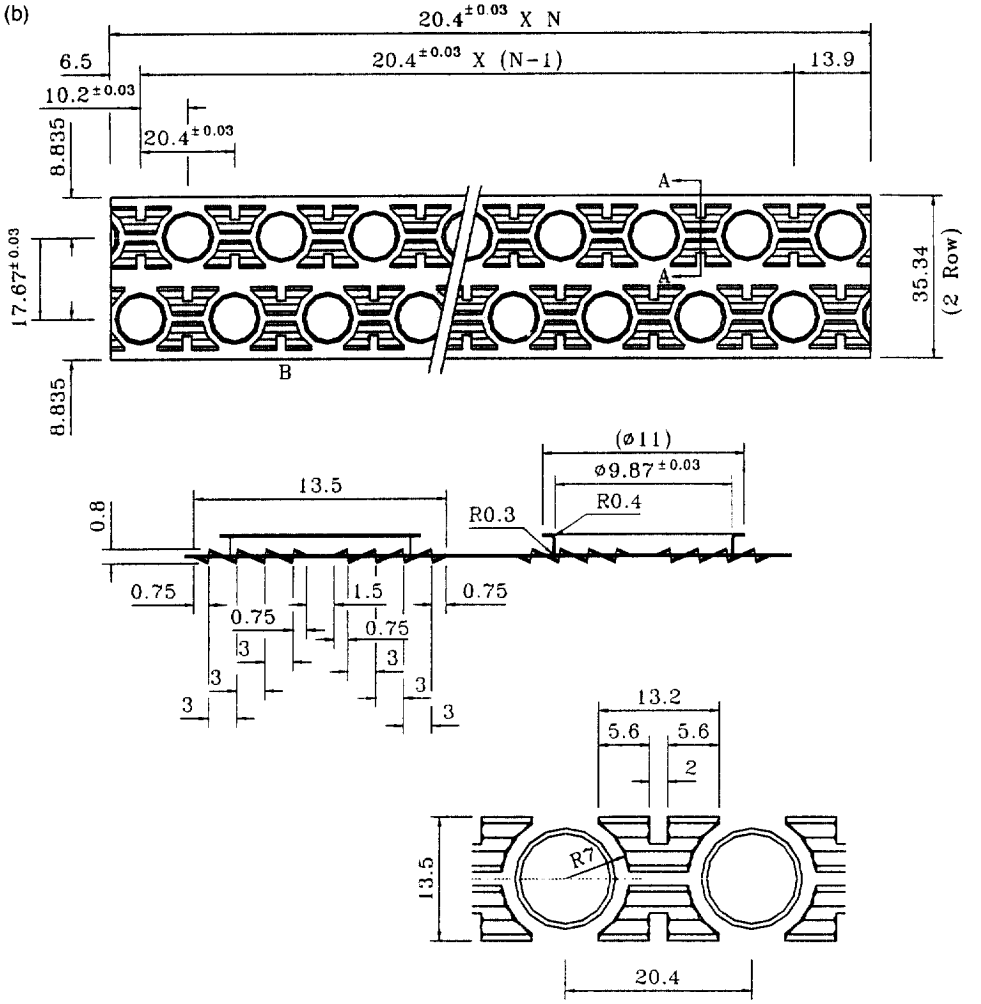

Fig. 1b. Detailed configuration of louver fin pattern (sample #7).

the modified correlation can predict the original data bank quite satisfactorily. Actually, 90.7% of the Rich data were predicted within ±15% compared to 95.3% by the Gray and Webb correlation ($Re_{D_c} \geqslant 2000$). For $Re_{D_c} < 2000$, the mean deviation is the same for both correlations. The proposed modified correlation gives excellent predictions with the present data in practical design conditions ($Re_{D_c} > 2000$). However, a considerable under-prediction still exists for $Re_{D_c} < 2000$. Further investigations are therefore needed to extend the range of the correlation.

The effect of hydrophilic coating on the heat transfer and pressure drop characteristics for the parallel louver fin pattern under completely dry conditions is shown in Fig. 5 (sample #2, #3, and #4). As seen, both heat transfer coefficients and pressure drops are virtually the same, regardless of the type of hydrophilic coating. Similar results for the anti-corrosion coating were also reported by Fu et al. [17].

Figure 6 gives the enhancement ratios for louver fin surface relative to the plain fin surface under completely dry conditions. The heat transfer enhancement ratio for the parallel louver (Fig. 1a), evaluated as $(h_{louver}/h_{plain}-1)$, is less than 5% for $V_{fr} = 0.3$ m s^{-1}, increases to a maximum value of 45% for $V_{fr} \approx 1.6$ m s^{-1}, and decreases slowly to 30% for $V_{fr} = 6.5$ m s^{-1}. The penalty of pressure drop ratio for the present parallel louver fin geometry is approximately 90–100% higher than that of plain surface. The enhancement ratios for the louver fin pattern in Fig. 1c) give a maximum enhanced ratio as $V_{fr} \approx 3$ m s^{-1}. For $Fp = 1.71$ mm, the value of $(h_{louver}/h_{plain}-1)$ is only 55–65% while the value of $(\Delta p_{louver}/\Delta p_{plain}-1)$ is more than 110%. The enhanced ratios are further reduced to 25–50% for $Fp = 1.22$

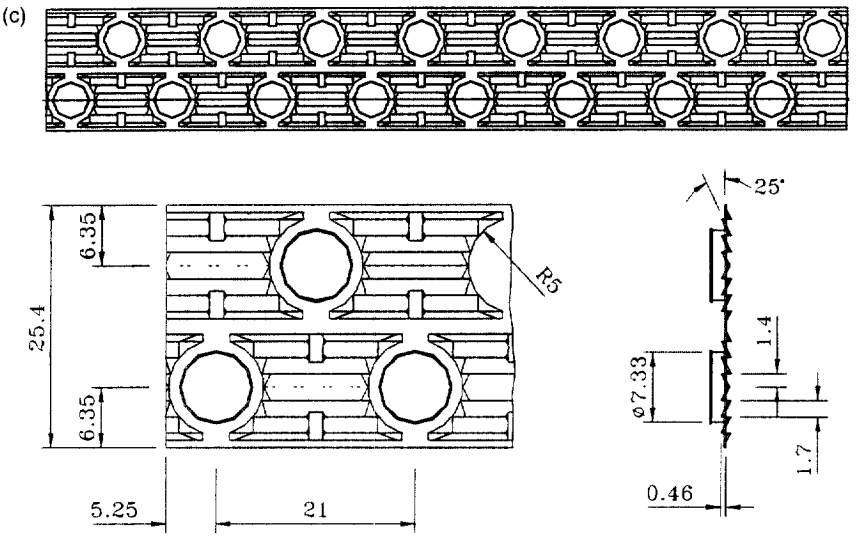

Fig. 1c. Detailed configuration of louvered fin pattern (samples #9 and #11).

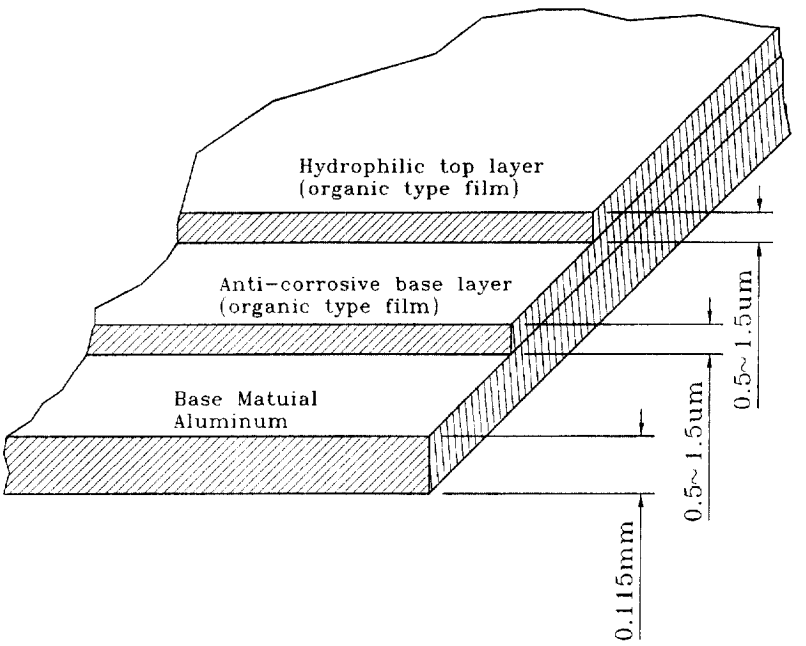

Fig. 2. Schematic of the composition of pre-coated surface.

mm and $V_{fr} > 1.0$ m s^{-1}. The increase of pressure drop, $(\Delta p_{louver}/\Delta p_{plain} - 1)$, is more than 140% for $V_{fr} > 6.0$ m s^{-1}. Converse to the heat transfer results, the pressure drop ratios show no 'maximum' phenomenon for the louver fin pattern of both Figs 1b and 1c, and increases with an increase of face velocity. For purposes of comparison, an estimated value of the enhanced ratio of Fig. 1c louver fin geometry having $Fp = 1.4$ mm is also given in Fig. 6. It is interesting to note that the enhancement ratio for the parallel louver is approximately 15% higher than that for the Fig. 1b and inclined louver fin patterns are about the same for $V_{fr} \leqslant 1.7$ m s^{-1}, while the parallel louver gives approximately 80% lower pressure drop. Note that the louver pitch of the parallel louver fin is one third that of the inclined louver fin in Fig. 1b. For $V_{fr} > 3$ m s^{-1}, the enhancement ratio of the parallel louver fin pattern are approximately 30–40% lower than that of the louver fin pattern of Fig. 1c for both heat transfer

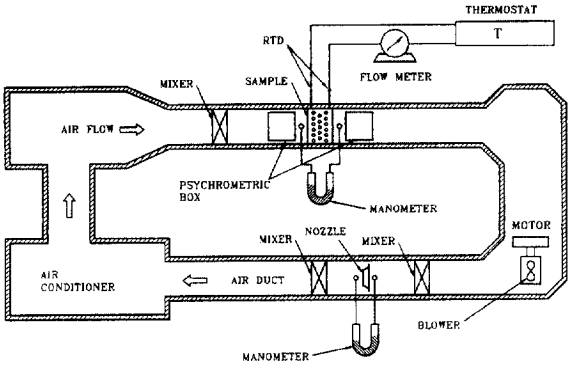

Fig. 3. Schematic of experimental setup.

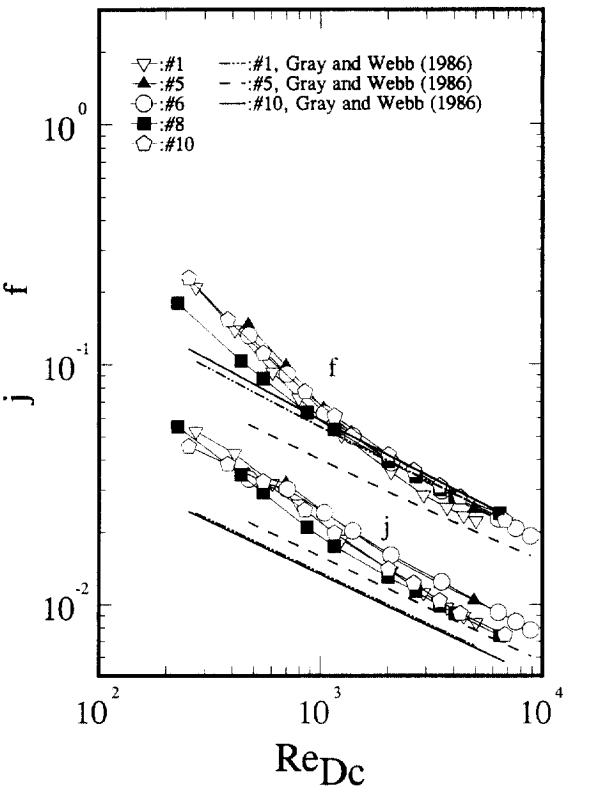

Fig. 4. Heat transfer and pressure drop for the plain fin samples.

coefficients and pressure drops. For the evaporators used for HVAC&R application, the frontal velocity, $V_{fr} < 2$ m s^{-1} usually.

The enhancement ratios for the louver fin pattern (Fig. 1b) are different from those of Fig. 1c. For $V_{fr} < 1.5$ m s^{-1}, the enhancement ratios for the two louver fin patterns are about the same. A noticeable reduction for Fig. 1b pattern is noted for $V_{fr} > 1.5$ m s^{-1}. A possible explanation about the differences may be related to the differences of louver angles. The louver angle for Fig. 1b is 15° compared to 25° for Fig. 1c. Webb and Trauger [18] found that at low Reynolds numbers, some of the air streams bypass the louvers and act as a 'duct flow' between the fin channels. Achaichia and Cowell [19] identified the flow pattern as 'fin directed flow' for low velocity region and 'louver directed flow' for the high Reynolds number region. For 'fin directed flow' at the low Reynolds number, there is no significant difference between the louver fin pattern in Fig. 1b, 1c, and even 1a. For higher frontal velocities, the 'louver directed' takes effect, and as indicated by the experimental data of Webb and Trauger [18], for a fixed value of L_p/F_p, the flow efficiency increases with increase of louver angle. Hence, the larger louver angles are beneficial, as shown in the Fig. 1c louver geometry.

For dehumidifying conditions, the sensible heat transfer coefficients for the present test samples of #1, #2, #3, and #4 are given in Fig. 7. As the surface temperatures are less than the corresponding inlet dew point temperatures, the surfaces are considered completely wet. The effect of hydrophilic coating on the sensible heat

Table 2
Summary of estimated uncertainties

Primary measurements		Derived quantities				
			Uncertainty $Re_{D_c} = 300$		Uncertainty $Re_{D_c} = 5000$	
Parameter	Uncertainty	Parameter	Dry	Wet	Dry	Wet
$\dot{m}_{air}$	0.3–1%	Re_{D_c}	±1.0%	±1.0%	±0.57%	±0.57%
$\dot{m}_w$	0.5%	Re_{d_c}	±0.73%	±0.73%	±0.73%	±0.73%
ΔP	0.5%	f	±16.7%	±10.7%	±1.4%	±1.0%
T_w	0.05 C	$\dot{Q}_w$	±3.5%	±4.95%	±1.22%	±1.52%
T_a	0.1 C	$\dot{Q}_a$	±5.5%	±7.5%	±2.4%	±3.4%
T	0.1 C	j	±11.4%	±14.4%	±4.6%	±6.5%

Table 3
Comparison of the proposed modified Gray and Webb correlation with the present experimental data and Rich [15, 16]

	Predictions by the modified Gray and Webb correlation			
	Present samples		Rich	
Deviation	$Re_{D_c} < 2000$	$Re_{D_c} \geq 2000$	$Re_{D_c} < 2000$	$Re_{D_c} \geq 2000$
±15%	20%	100%	85.3%	90.7%
Average deviation	−27.2%	−2.1%	3.7%	4.3%

Table 4
Comparison of the original Gray and Webb correlation with the present experimental data and Rich [15, 16]

	Predictions by the Gray and Webb correlation			
	Present samples		Rich	
Deviation	$Re_{D_c} < 2000$	$Re_{D_c} \geq 2000$	$Re_{D_c} < 2000$	$Re_{D_c} \geq 2000$
±15%	Nil	Nil	85.3%	95.3%
Average deviation	−43%	−23.7%	0.4%	0.8%

Average deviation

$$= \frac{1}{K}\left(\sum_{1}^{K} \frac{j_{\text{pred}} - j_{\text{exp}}}{j_{\text{exp}}}\right) \times 100\%.$$

K: Number of data points.

transfer characteristics are negligible. For a frontal velocity less than 0.7 m s^{-1}, the sensible heat transfer coefficients for the parallel louver fin surface are nearly the same as those of plain fin surfaces. This phenomenon is quite different from that of a dry surface. In dehumidifying operation and low face velocity, the water condensate may block the louver and reduce the potential performance of the enhanced surfaces. This suggests a lower enhancement level for slit fin patterns under dehumidifying conditions at low velocities. Note that the sensible heat transfer coefficients are also independent of the inlet condition for the test surface. For inlet relative humidity of 50% and 85%, there are no detectable differences between the sensible heat transfer coefficients for both plain and louver fin patterns. In addition, the pressure drops are also independent of inlet conditions for the surfaces without hydrophilic coating (sample #1 and #2). Similar test results for the plain fin geometry were also reported by Wang et al. [11]. For an inlet relative humidity of 85%, the pressure drops of the hydrophilic coating surface reveal a dependence of inlet conditions. Comparing with the un-coated surfaces, 25–40% lower pressure drops are shown for the hydrophilic coating surfaces at an inlet condition of 50%. However, the pressure drops for the hydrophilic surfaces are approximately 15–30% lower than those of uncoated surfaces for RH = 85%. Possible explanations of this phenomenon are described as follows. For the un-treated surfaces, the water contact angle is very large; the condensate retention occurs for both the 50% and 85% inlet conditions. The condensate retention causes air flow in a series of 'contraction-expansion' states. Since a significant condensate retention phenomenon exists for RH = 50% and 85%, no detectable differences of pressure drops are seen for the uncoated surfaces under completely wet condition. Conversely to the uncoated surfaces, the lower contact angles for the hydrophilic coating surfaces may reduce the condensate retention and cause the condensate film forms on the surfaces. As a results, for a higher RH, higher latent load may result in thicker film thickness, accelerate the airflow within the heat exchangers, and increase the pressure drops. Thus, the hydrophilic coating surfaces revealed a dependence of the inlet conditions.

Dry/wet cycling tests were conducted on two heat exchangers geometries to examine the durability of the

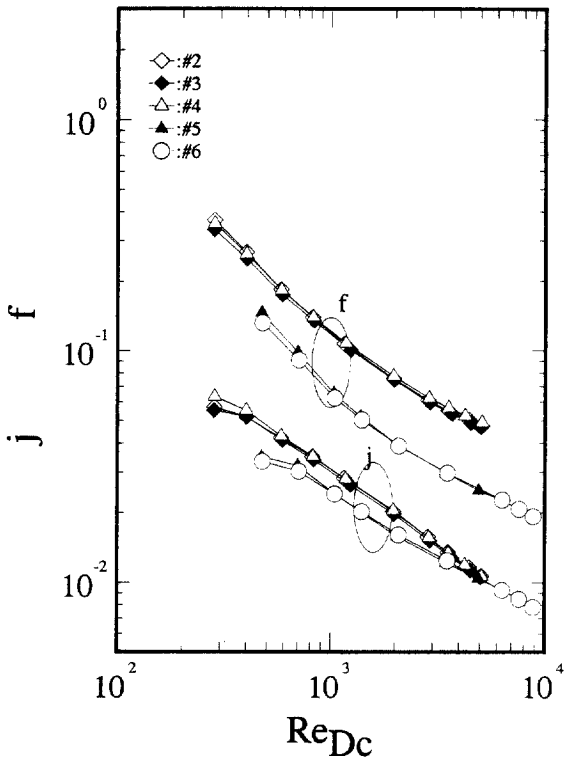

Fig. 5. Effect of the hydrophilic coating on the heat transfer and friction characteristics under completely dry test conditions.

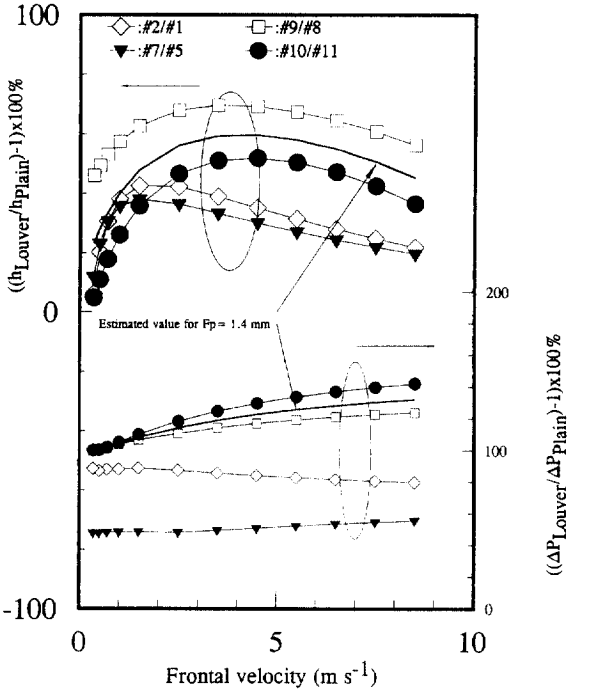

Fig. 6. Enhancement ratios for louver fin patterns under completely dry conditions.

hydrophilic coating (samples #3 and #4). The dry/wet cycle is similar to the procedure reported by Mimaki [4] that consists of 15 minutes of spray water to the heat exchangers and then hung up to dry by a fan for 15 minutes. After a hundred dry/wet cycles, we re-examined the thermal-hydraulic performance of the coated surfaces. It was found that no significant degradation of the performances for the coated surfaces was seen.

The sensible heat transfer coefficients and pressure drops for samples #5, #6, #7, #8, #9, #10, and #11 for fully wet state are illustrated by Figs 8 and 9 (RH = 85%). Again, $V_{fr} < 0.7$ m s^{-1}, the heat transfer coefficients for the louver fin (Fig. 1b) and plain fin are virtually the same. It seems that the enhancement ratios of the louver fin patterns (Fig. 1b,c) of the sensible heat transfer coefficients are sensitive to the louver angle. For a louver angle of 15°, the enhancement is less than 20% for $V_{fr} = 2$ m s^{-1}. For a louver angle of 25° (Fig. 1c), the enhancement is approximately 30%. The corresponding increase of pressure drop (relative to its plain fin counterpart at wet operation condition), are approximately 80% higher for Fig. 1b and 100% higher for Fig. 1c.

The dehumidifying process involves heat and mass transfer simultaneously; if mass transfer data are unavailable, it is convenient to employ the analogy

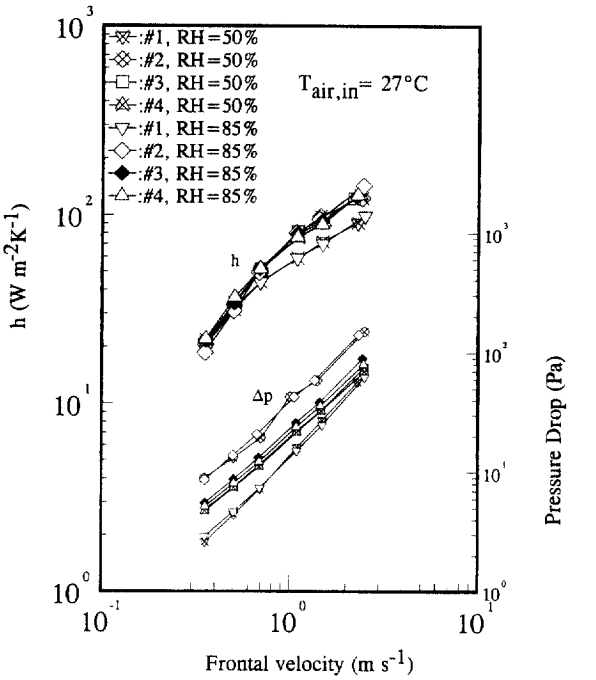

Fig. 7. Effect of the hydrophilic coating on the heat transfer and friction characteristics under completely wet test conditions.

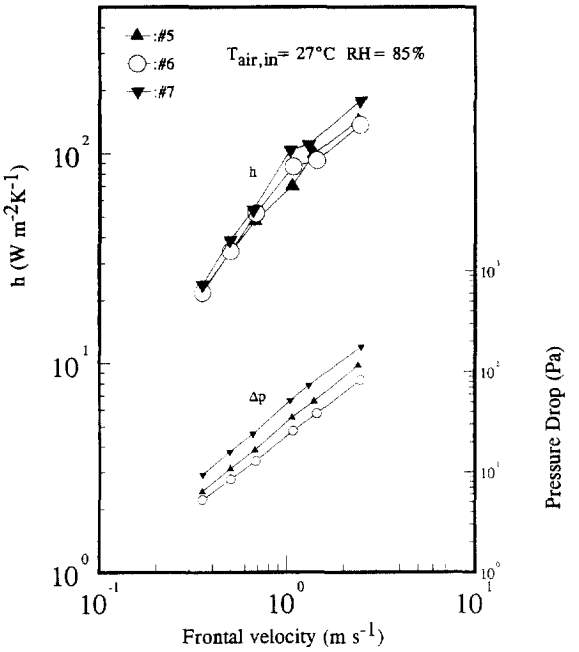

Fig. 8. Sensible heat transfer coefficients and pressure drops for samples #5, #6, and #7 under completely wet test conditions.

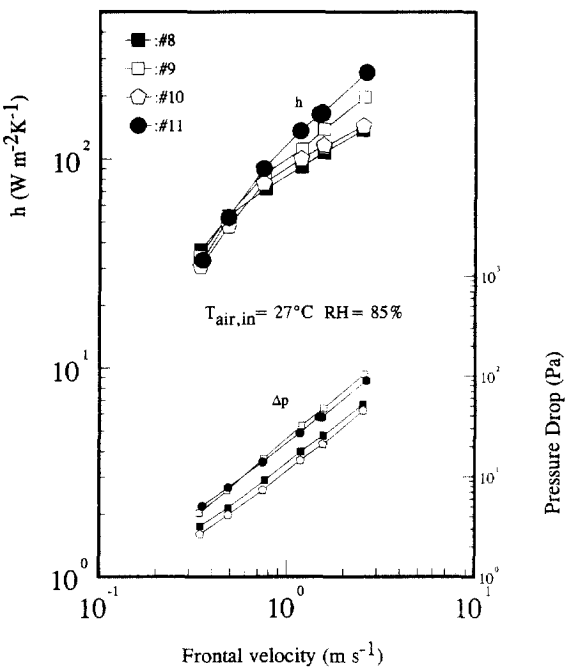

Fig. 9. Sensible heat transfer coefficients and pressure drops for samples #8, #9, #10, and #11 under completely wet test conditions.

between heat and mass transfer, because heat conduction and mass diffusion in a liquid are governed by physical laws of the same mathematical form, such that

$$\frac{h_{co}}{h_d C_p P_{AM}} \approx 1 \tag{6}$$

P_{AM} is the logarithmic mean density factor, and is given by

$$P_{AM} = \frac{p}{p_{AL}}\left(\frac{\ln\left(\frac{\rho_{AL}}{\rho_{AO}}\right)}{(\rho_{AL}-\rho_{AO})}\right) \tag{7}$$

where ρ_{AL} denotes the mean air density at the bulk fluid, and ρ_{AO} is mean air density evaluated at the interface. The term P_{AM} in equation (7) approximately equals unity for dilute mixtures like water vapor in air near the atmospheric pressure (temperature well-below corresponding boiling point). Therefore, equation (6) can be simplified to yield

$$\frac{h_{co}}{h_d C_p} \approx 1. \tag{8}$$

The validity of equation (8) relies heavily on the mass transfer rate. The experimental data of Hong [5] indicated that this value is between 0.7–1.1; Seshimo et al. [20] gave a value of 1.1. Eckels and Rabas [21] also reported the relevance in their plain fin-and-tube heat exchangers. We found that the values of $h_{c,o}/(h_d C_p)$ were generally 0.75–1.0. However, Idem et al. [22] reported values ranged 1.3–2.1 for the baffled heat exchangers. Idem and Goldschmidt [23] argued that at high rates of condensation, the presence of thick condensate layers may alter the adjacent thermal and viscous boundary layer, thereby to show deviations from equation (8). Further examinations of the test conditions by Idem and Goldschmidt [23] showed that their inlet air temperatures ($T_{air,in} \approx 93.5$°C, $T_{water} \approx 15$°C) were much higher than in previous investigations. Eventually, the corresponding fin surface temperature would be much higher than other investigators, and so the inclusion of P_{AM} in equation (8) is needed. Hence, the experimental data of Idem et al. [22] can still be described by equation (6).

Based on the present test results, the ratio of $h_{c,o}/(h_d C_p)$ can be correlated as

$$\frac{h_{c,o}}{h_d C_p} = 0.57 Re_{D_h}^{0.07} \tag{7}$$

and

$$Re_{D_h} = \frac{4A_c L}{A_o}. \tag{8}$$

The present test result is analogous to those reported by Hong [5]. The measured mass transfer coefficients slightly increased with the velocities. For lower velocities, the heat and mass transfer analogy slightly overpredicts the results, which is analogous to the findings of Hong [5].

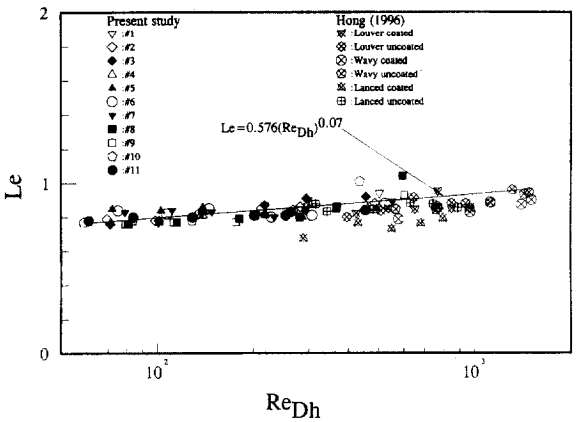

Fig. 10. $h_{c,o}/h_d C_p$ vs Reynolds number for the present test samples and Hong (1996).

Figure 10 shows the ratios of $h_{c,o}/(h_d C_p)$ for the present test samples and those of Hong [5]. Good predictive ability of equation (7) with the test data of Hong [5] is shown.

4. Conclusions

Heat and mass transfer characteristics for 11 samples of louver fin pattern are reported in the present study. It is shown that the enhancement ratios decrease with decrease of fin pitch. A slight modification to the Gray and Webb correlation [14] is proposed, which gives very good agreement with the data for $V_{fr} > 2$ m s^{-1}, and also gives satisfactory predictions of the plain fin data reported by Rich [15, 16].

For a completely dry surface condition, the hydrophilic coating has a negligible effect on the thermal-hydraulic performance. For completely wet test conditions, the hydrophilic coating has a negligible effect on the sensible heat transfer coefficients, and the pressure drops are approximately 15–40% lower than those without coating. In addition, the pressure drops for hydrophilic coated surfaces are sensitive to the inlet conditions. Converse to the hydrophilic coating surfaces, the pressure drops for those without coating, are independent of the inlet conditions.

The ratio of $h_{c,o}/(h_d C_p)$ is found to be around the order of unity. A brief survey of previous investigations and the present study of fin-and-tube heat exchangers substantiate the present results. However, for higher mass transfer rate, evaluations of P_{AM} should be included.

Acknowledgements

The authors are indebted to the Energy R&D foundation funding from the Energy Commission of the Ministry of Economic Affairs, Taiwan, for supporting this study.

References

[1] Chang WR, Wang CC, Tsi WC, Shyu RJ. Air side performance of louver fin heat exchanger. Proc of the 4th ASME/JSME Thermal Engineering Joint Conference 1995;4:367–72.

[2] Wang CC, Chang YP, Chi KU, Chang YJ. An experimental study of heat transfer and friction characteristics of typical louver fin and tube heat exchangers. Int J of Heat and Mass Transfer 1998;41(4–5):817–22.

[3] Wang CC, Chang YP, Chi KU, Chang YJ. A study of non-redirection louver fin-and-tube heat exchangers. Proceedings of Institute of Mechanical Engineering, Part C, Journal of Mechanical Engineering Science, 1998;212:1–14.

[4] Mimaki M. Effectiveness of finned tube heat exchanger coated hydrophilic-type film. ASHRAE paper #3017 presented at January meeting, 1987.

[5] Hong K. Fundamental characteristics of dehumidifying heat exchangers with and without wetting coating. Ph.D. thesis. Department of mechanical engineering, the Pennsylvania State University, U.S.A., 1996.

[6] ASHRAE Standard 41.1-1986, Standard Method for Temperature Measurement. Atlanta: American Society of Heating, Refrigerating and Air-Conditioning Engineers, Inc, 1986.

[7] ASHRAE Standard 41.2-1987, Standard Methods for Laboratory Air-flow Measurement. Atlanta: American Society of Heating, Refrigerating and Air-Conditioning Engineers, Inc, 1987.

[8] ASHRAE Standard 33-78. Method of Testing Forced Circulation Air Cooling and Air Heating Coils. Atlanta: American Society of Heating, Refrigerating and Air-Conditioning Engineers, Inc, 1978.

[9] Moffat RJ. Describing the uncertainties in experimental results. Experimental Thermal and Fluid Science 1988;1:3–17.

[10] Wang CC, Hsieh YC, Chang YJ, Lin YT. Sensible heat and friction characteristics of plate fin-and-tube heat exchangers having plane fins. Int J of Refrigeration 1996;19(4):223–30.

[11] Wang CC, Hsieh YC, Lin YT. Performance of plate finned tube heat exchangers under dehumidifying conditions. ASME Journal of Heat Transfer 1997;119:109-17.

[12] Threlkeld JL. Thermal Environmental Engineering, New York: Prentice-Hall, Inc, 1970.

[13] Myers RJ. The effect of dehumidification on the air-side heat transfer coefficient for a finned-tube coil, M.S. Thesis, University of Minnesota, Mineapolis, 1967.

[14] Gray DL, Webb RL. Heat transfer and friction correlations for plate finned-tube heat exchangers having plain fins. Proc 8th Heat Transfer Conference, 2745–50, 1986.

[15] Rich DG. The effect of fin spacing on the heat transfer and friction performance of multi-row, plate fin-and-tube heat exchangers. ASHRAE Transactions 1973;79(2):137–45.

[16] Rich DG. The effect of the number of tube rows on heat

transfer performance of smooth plate fin-and-tube heat exchanger. ASHRAE Transactions 1975;81(1):307–17.

[17] Fu WL, Wang CC, Chang CT. Effect of anti-corrosion coating on the thermal characteristics of a louvered finned heat exchanger under dehumidifying condition. ASME HTD-Vol. 320/PID-Vol. 1. Advances in Enhanced Heat/Mass Transfer and Energy Efficiency, 1995, p. 75–81.

[18] Webb RL, Trauger P. Flow structure in the louvered fin heat exchanger geometry. Exp Thermal and Fluid Sci 1991;4:205–17.

[19] Achaichia A, Cowell TA. Heat transfer and pressure drop characteristics of flat tube and louvered plate fin surfaces. Exp Thermal and Fluid Sci 1988;1:147–57.

[20] Seshimo Y, Ogawa K, Marumoto K, Fujii M. Heat and mass transfer performances on plate fin and tube heat exchangers with dehumidification. Transactions JSME 1988;54[499]:716–21.

[21] Eckels PW, Rabas TJ. Dehumidification: On the correlation of wet and dry transport process in plate finned-tube heat exchangers. ASME Journal of Heat Transfer 1987;109:575–82.

[22] Idem SA, Jacobi AM, Goldschmidt VW. Heat transfer characterization of a finned-tube heat exchanger (with and without condensation). ASME Journal of Heat Transfer 1990;112:64–70.

[23] Idem SA, Goldschmidt VW. Sensible and latent heat transfer to a baffled finned-tube heat exchanger. Heat Transfer Engineering 1993;14(3):26–35.